Front. Optoelectron. 2020, 13(2): 149–155
https://doi.org/10.1007/s12200-020-1057-4

RESEARCH ARTICLE

Fe_3O_4 nanoparticle-enabled mode-locking in an erbium-doped fiber laser

Xiaohui LI (✉)[1], Jiajun PENG[1], Ruisheng LIU[1,2], Jishu LIU[1], Tianci FENG[1], Abdul Qyyum[1], Cunxiao GAO (✉)[2], Mingyuan XUE[2], Jian ZHANG[2]

1 College of Physics and Information Technology, Shaanxi Normal University, Xi'an 710119, China
2 State Key Laboratory of Transient Optics and Photonics, Xi'an Institute of Optics and Precision Mechanics, Chinese Academy of Sciences, Xi'an 710119, China

Abstract In this paper, we have proposed and demonstrated the generation of passively mode-locked pulses and dissipative soliton resonance in an erbium-doped fiber laser based on Fe_3O_4 nanoparticles as saturable absorbers. We obtained self-starting mode-locked pulses with fundamental repetition frequency of 7.69 MHz and center wavelength of 1561 nm. The output of a pulsed laser has spectral width of 0.69 nm and pulse duration of 14 ns with rectangular pulse profile at the pump power of 190 mW. As far as we know, this is the first time that Fe_3O_4 nanoparticles have been developed as low-dimensional materials for passive mode-locking with rectangular pulse. Our experiments have confirmed that Fe_3O_4 has a wide prospect as a nonlinear photonics device for ultrafast fiber laser applications.

Keywords Fe_3O_4, rectangular pulse, dissipative soliton, erbium-doped fiber, nonlinear photonics

1 Introduction

The mode-locked pulse fiber lasers have many important applications in nonlinear optics, fiber optic communication, optical time domain clock, laser processing, and optical measurement [1,2]. Popular methods to implement a mode-locked operation include active [3,4] and passive mode-locking [5–8]. The appearance of new optical saturable absorbers promotes the development of passively mode-locked lasers. Compared with traditional mode-locking methods, new materials expand research on pulsed lasers due to their characteristic wavelength independence, high heat dissipation, and high laser damage threshold [9–1]. Semiconductor saturable absorber mirrors [13], carbon nanotubes [14,15], graphene [16–18], bismuthene [19], topological insulators [20,21], transition metal sulfides [22–27], and black phosphorus [28] have been reported and demonstrated for the applications of mode-locking. When carbon nanotubes are used as saturable absorbers, their sizes extremely affect the absorption wavelength and increase the loss of unsaturable absorption [15]. Graphene has a weaker modulation of light for its weak absorption [17]. The tapper insulator cannot achieve higher power laser output as it has a low damage threshold [29,30]. Fe_3O_4 has obvious nonlinear sensitivity as a transition metal sulfide [31–33]. As its response time is within tens of picoseconds, it can be applied to many large nonlinear optical responses [34,35]. In previous reports, the band gap of Fe_3O_4 was observed, which was considered as semiconductor and its band gap energy changed with the particle size [36]. The imaginary part of the third-order nonlinear magnetic susceptibility enables nonlinear absorption, which allows the Fe_3O_4 nanoparticles to act as a saturable absorber of the fiber laser to generate pulses. Simultaneously, the real part of the third-order nonlinear polarizability of the nanoparticle achieves the optical Kerr effect. The nanoparticles of Fe_3O_4 can be used as nonlinear medium [34–36]. Mode-locked fiber lasers based on Fe_3O_4 nanoparticles have been demonstrated. Li et al. reported a 1558 nm mode-locked fiber laser based on Fe_3O_4 nanoparticles as a saturated absorber [37]. Bai et al. used ferroferric-oxide (Fe_3O_4) nanoparticles (FONPs) as the saturable absorber (SA) to realize the Q-switch operation in an erbium-doped fiber laser (EDFL), where the minimum pulse duration was approximately 3.2 μs [33]. Yang et al. reported the use of Fe_3O_4 nanoparticles for Q-switched a tunable mid-infrared (Mid-IR) Dy^{3+}-doped ZBLAN fiber laser around 3 μm [38]. Recently, Liu et al.

Received June 8, 2020; accepted June 17, 2020

E-mails: lixiaohui@snnu.edu.cn (X. Li), cxgao@opt.ac.cn (C. Gao)

reported the realization of nanosecond pulses in an EDFL using FONPs as SA. Nevertheless, the SAs with Fe_3O_4 nanoparticles have been focused primarily on Q-switched fiber lasers [39].

In this work, we demonstrated the mode-locked pulse output of an EDFL based on Fe_3O_4. The Fe_3O_4 nanoparticles are deposited on the end plane of the fiber patch cord by liquid deposition. The light absorption between the transmitted light field and the Fe_3O_4 nanoparticles in the single-mode fiber (SMF) achieves the saturation absorption effect. The laser polarization state was adjusted each time and the laser pulse was self-started at a pump power of 70 mW, where the repetition frequency was 7.69 MHz. The simple experimental setup is beneficial to engineering and industrialization. The experimental results show that Fe_3O_4 can be used as a nonlinear optical modulation material like other optical materials, which has far-reaching influence on the design and development of pulse lasers.

2 Experimental results

The Fe_3O_4 nanoparticles have high third-order optical nonlinearity, a large nonlinear optical response, and fast response time. The recovery time for Fe_3O_4 nanoparticles was assessed at 18–30 ps [36] and classified as a semiconductor material (with a band gap of ~ 0.3 eV), which can be modulated by tuning the nanoparticle diameter [40]. To prepare Fe_3O_4 nanoparticles, we first took some Fe_3O_4 powders and acetone into a reagent bottle and placed them in an ultrasonic machine of 40 kHz (KQ-400 KDE) for 4 h. After one hour, the solution and the supernatant were taken out from the machine. Then, we get the SA based on the Fe_3O_4 nanoparticle membrane, which is a new 2D material. Figure 1 shows the characteristics of the material after magnifying the SA by scanning electron microscope (SEM). It shows the image of the magnification of 24000. We observe that Fe_3O_4 nanoparticles are nearly spherical and have a diameter of about 200 nm.

The nonlinear absorption characteristics of Fe_3O_4 used in the experiment were measured by the double-balanced detection method [5]. Figure 2 shows the measured

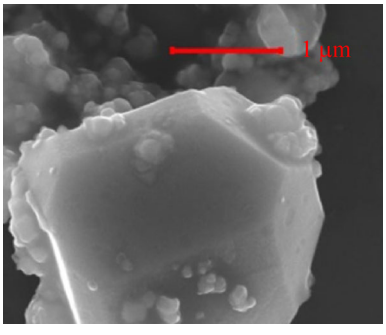

Fig. 1 SEM image of Fe_3O_4

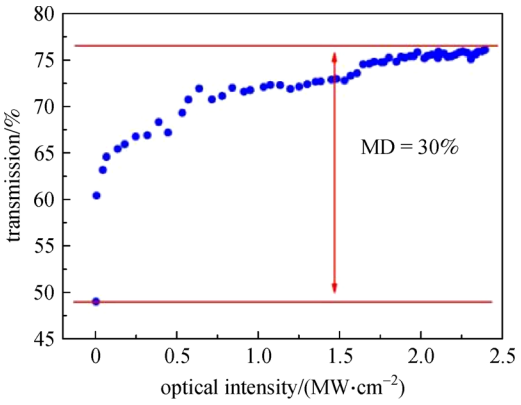

Fig. 2 Nonlinear transmission of Fe_3O_4-SAs

transmission curve. We have also observed that the modulation depth (MD) is about 30%. The seed source femtosecond laser used in the measurement process has a center wavelength of 1560.3 nm, a repetition frequency of 12.34 MHz, and pulse duration of 644 fs.

In this experiment, we used a SMF patch cord. The deposited solution formed a thin film of liquid on the FC/PC fiber end. The dispersion completely evaporated within 5 to 10 min. The solute Fe_3O_4 nanoparticles were attached to the fiber end. After repeating this process for a few times, some layers of Fe_3O_4 nanolayers eventually were formed on the end of the FC/PC patch cord after connecting two fiber taps by a flange. We integrated it with the laser cavity.

Figure 3 shows the principal structure of the fiber laser used in the experiment. The ring laser cavity includes an specific length of gain fiber, a 980/1550 wavelength division multiplexer (WDM), a polarization-independent fiber isolator (ISO), a fiber output coupler (OC), a squeezer polarization controller, and a standard single-mode FC/PC

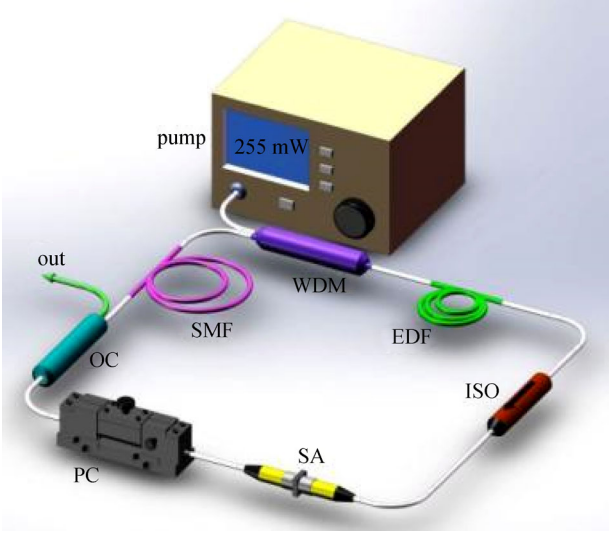

Fig. 3 Fiber laser with Fe_3O_4 as mode-locker

optical fiber patch cord, whose FC/PC end was deposited with Fe_3O_4 nanoparticles as a SA. In this experiment, a tabletop laser with the wavelength of 980 nm at center was used as pump source, whose power could be adjusted from 0 to 255 mW.

The erbium-doped fiber (EDF; NUFERN, EDFC-980-HP, USA) was used as a gain fiber with a length of 3.3 m, and the absorption at 980 nm is about 3 dB/m. We inserted a FC/PC optical fiber patch cord with the end deposited with Fe_3O_4 nanoparticles into the cavity by a flange. The polarization-independent optical isolator ensures the one-way transmission of light in the laser cavity. A polarizer controls the different polarization states of the light in the cavity. The output coupler with output ratio of 10:90 connects measuring equipment, whose branch of 10% is used as the output, and branch of 90% is connected back to the fiber ring. The total length of the laser cavity was measured to be ~23.5 m, containing ~3.3 m long EDF and ~20.2 m long SMF, which consists of pigtails of optical devices and other fibers, except EDF, in the cavity. At 1550 nm, the dispersion parameters D are −16 ps/(nm·km) for EDF and 17 ps/(nm·km) for SMF. The total net dispersion of the cavity is ~0.38 ps^2. So, it is possible to achieve a soliton mode-locked operation in the fiber laser. During the experiment, we detected the output spectrum of the laser by a spectrum analyzer (YOKOGAWA, AQ6375, Japan). The pulse train is observed by a photodetector (THORLABS, DET08CFC, 2 GHz, USA) and a digital oscilloscope (RIGOL, DS4054, 1 GHz, China). The radio-frequency spectrum is observed by a spectrum analyzer (AGILENT, E4447A, USA) and the output power is recorded by a hand-held optical power meter (JOINWIT, JW3208, China).

Self-start mode-locked pulses could be observed at a pump power of 70 mW. The pulse train tends to stabilize and the output power increases with the pump power. The slope of the curve is ~3.16% as shown in Fig. 4(a). The pulse disappears when the power decrease to 65 mW and the continuous wave light outputs due to the hysteresis effect [41].

3 Results and discussion

Figure 5(a) shows an output spectrum with a center wavelength of 1561 nm and the spectral width of 0.69 nm at the pump power of 190 mW. The outline of the spectral image is M-shaped and the shape of its peak appears as concave. The whole spectrum exhibits an axisymmetric characteristic, extending to both sides from the M-shaped pit point and the peak of the spectral curve undulating corresponding sideband. The appearance of the spectrum with an M-shaped profile is a typical characteristic of dark solitons operation in the cavity corresponding to the waveform below the baseline as shown in Fig. 5(b) [42,43]. These sidebands represent the properties of the optical pulse output and are often called Kelly-sidebands. The entire spectrum curve also presented the feature of dissipative soliton resonance. Figure 5(b) shows the evolution of the spectrum with an increase in pump power. If the pump power increases, the gain will increase as rectangular pulse will be formed. The wavelength of the long wave spectrum will increase, while the wavelength of shorter spectrum will gradually decrease [44]. The pulse characteristic of the rectangular square wave is that it drops approximately 20 ns after reaching its saturation point. The spectral width varies from ~0.69 to 1.05 nm and the leftmost spectral peak is clearly enhanced due to the Kelly effects with the pump power ranging from 190 to 240 mW. However, the overall outline of the spectrum remains unchanged. We observed the single rectangular pulse duration of about 14 ns at pump power of 190 mW as shown in Fig. 5(c). The formation of this type of pulse is related to the dissipative soliton resonance in the cavity [45]. The reason behind the formation of rectangular wave without flat top is that the dynamic saturation effect of the gain in the laser cavity causes the pulses to receive different gains at the front and rear edges [46,47].

Figure 5(d) shows the evolution of the width of the pulse with the increase in pump power. The quality of rectangular pulse will be improved with a flat top in the future work. The pulse duration increases from 14 to 20 ns

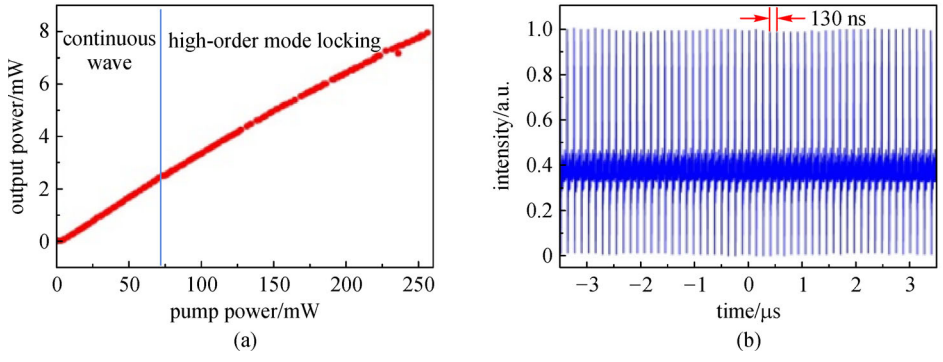

Fig. 4 (a) Output power as function of the pump power. (b) Pulse train at pump power of 190 mW, the fundamental repetition frequency is 7.69 MHz at pump power of 190 mW. The interval of two pulses is ~130 ns

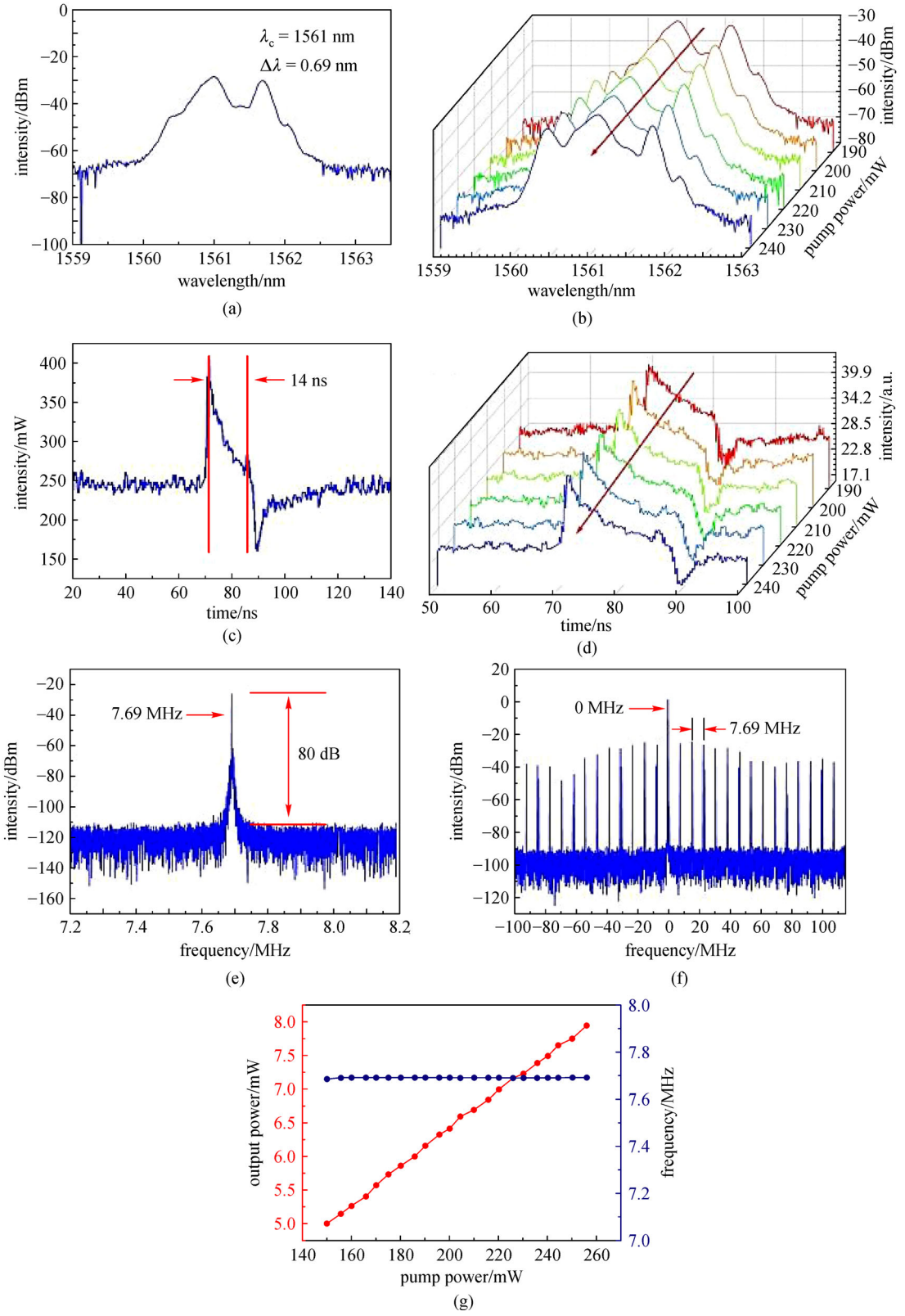

Fig. 5 (a) Output spectrum at the pump power of 190 mW. (b) Evolution of spectrum with pump power from 190 to 240 mW. (c) Single pulse at the pump power of 190 mW. (d) Evolution of single pulse with pump power from 190 to 240 mW. (e) RF-spectrum of single frequency at the pump power of 190 mW ((e) is a magnified interception of (f)). (f) RF of frequency at the pump of 190 mW. (g) Evolutions of frequency and output power with pump power

with the increase in pump power from 190 to 240 mW, which is similar to the previously reported results [48–50]. This phenomenon also shows a feature of dissipative soliton resonance. We can observe that the pulse duration becomes wider according to the changing trend of spectra. We can see that when the maximum pump power is 240 mW, the rectangular pulse remains unaffected. Here, we demonstrate that Fe_3O_4, as a SA, shows good compatibility with ultrafast fiber laser. Figure 5(e) shows the radio-frequency (RF) spectrum of the pulse laser with a center frequency of 7.69 MHz, a scan width of 1 MHz, and a resolution of 150 Hz at the pump power of 190 mW. Figure 5(f) shows that the frequency interval between two peaks is same as round trip frequency of the laser cavity with pump power of 190 mW, which shows that the resonant cavity achieves mode-locking. The bandwidth and resolution measured in the experiment are different. So, there are some noises at the base [51]. Figure 5(g) shows evolutions of repetition rate of the pulse laser with pump power. The repetition rate of pulses does not change with change in pump power. Autocorrelation trace cannot be measured because the pulse width is at a nanosecond scale. In the process of pulse width broadening, the rectangular pulses capture the weak pulse generated by the continuous wave, which leads to the soliton phenomenon [52]. Moreover, the mode-locked pulse is realized by Fe_3O_4 SA, the magnetic nanomaterial deposited on the end of patch cord is wiped off by alcohol. When the optical path was connected again at the pump laser power of 190 mW, no pulse was obtained. Then, polarization controller is adjusted and the power is changed from the highest to the lowest, but no pulse output appears. This confirms that Fe_3O_4 enables pulse mode-locking and it is a potential optical material that will play an important role in the field of laser mode-locking in the future.

4 Conclusions

We have observed passively mode-locked pulses in the EDF fiber laser based on Fe_3O_4 nanoparticles as the saturable absorber, which is deposited on the end of the fiber patch cord. The operation of the laser pulse with a repetition frequency of 7.69 MHz is achieved. When the pump power is 190 mW, a rectangular pulse is obtained. The change of pulse width is characterized by dissipative soliton resonance. The pulse width increases with the increase of pump power, but the intensity remains unaffected. The rectangular square wave is realized for the first time based on Fe_3O_4 nanoparticles. The phenomenon for dissipative soliton resonance will provide a new basis to the future research of soliton [53]. We can expect the potential applications of Fe_3O_4 in nonlinear optics and ultrafast photonics.

Acknowledgements This research was supported by the National Natural Science Foundation of China (Grant No. 61605106), Funded projects for the Academic Leader and Academic Backbones, Shaanxi Normal University (No. 18QNGG006), Shaanxi International Cooperation Project (No. 2020KW-005), Starting Grants of Shaanxi Normal University (Nos. 1112010209 and 1110010717), Open Research Fund of State Key Laboratory of Transient Optics and Photonics, Chinese Academy of Sciences (No. SKLST201809), Fundamental Research Funds for the Central Universities (Nos. GK201802006 and 2018CSLY005).

Disclosures The authors declare no conflicts of interest.

References

1. Oktem B, Ülgüdür C, Ilday F Ö. Soliton–similariton fibre laser. Nature Photonics, 2010, 4(5): 307–311
2. Kobtsev S, Kukarin S, Smirnov S, Turitsyn S, Latkin A. Generation of double-scale femto/pico-second optical lumps in mode-locked fiber lasers. Optics Express, 2009, 17(23): 20707–20713
3. Tang M, Tian X, Shum P, Fu S, Dong H, Gong Y. Four-wave mixing assisted self-stable 4 ×10 GHz actively mode-locked erbium fiber ring laser. Optics Express, 2006, 14(5): 1726–1730
4. Liu J S, Li X H, Guo Y X, Qyyum A, Shi Z J, Feng T C, Zhang Y, Jiang C X, Liu X F. $SnSe_2$ nanosheets for subpicosecond harmonic mode-locked pulse generation. Small, 2019, 15(38): 1902811
5. Greer E J, Smith K. All-optical FM mode-locking of fibre laser. Electronics Letters, 1992, 28(18): 1741
6. Cundiff S, Collings B, Knox W. Polarization locking in an isotropic, modelocked soliton Er/Yb fiber laser. Optics Express, 1997, 1(1): 12–21
7. Collings B C, Bergman K, Knox W H. Stable multigigahertz pulse-train formation in a short-cavity passively harmonic mode-locked erbium/ytterbium fiber laser. Optics Letters, 1998, 23(2): 123–125
8. Moenster M, Glas P, Steinmeyer G, Iliew R, Lebedev N, Wedell R, Bretschneider M. Femtosecond Neodymium-doped microstructure fiber laser. Optics Express, 2005, 13(21): 8671–8677
9. Wu K, Chen B, Zhang X, Zhang S, Guo C, Li C, Xiao P, Wang J, Zhou L, Zou W, Chen J. High-performance mode-locked and Q-switched fiber lasers based on novel 2D materials of topological insulators, transition metal dichalcogenides and black phosphorus: review and perspective. Optics Communications, 2018, 406: 214–229
10. Yang T, Lin H, Jia B. Two-dimensional material functional devices enabled by direct laser fabrication. Frontiers of Optoelectronics, 2018, 11(1): 2–22
11. Choi S, Jeong H, Hong B, Rotermund F, Yeom D. All-fiber dissipative soliton laser with 10.2 nJ pulse energy using an evanescent field interaction with graphene saturable absorber. Laser Physics Letters, 2014, 11(1): 015101
12. Liu X, Cui Y, Han D, Yao X, Sun Z. Distributed ultrafast fibre laser. Scientific Reports, 2015, 5(1): 9101
13. Haiml M, Grange R, Keller U. Optical characterization of semiconductor saturable absorbers. Applied Physics B, Lasers and Optics, 2004, 79(3): 331–339
14. Yamashita S, Inoue Y, Maruyama S, Murakami Y, Yaguchi H, Jablonski M, Set S Y. Saturable absorbers incorporating carbon nanotubes directly synthesized onto substrates and fibers and their

application to mode-locked fiber lasers. Optics Letters, 2004, 29 (14): 1581–1583
15. Liu H H, Chow K K. Dark pulse generation in fiber lasers incorporating carbon nanotubes. Optics Express, 2014, 22(24): 29708–29713
16. Xin W, Liu Z B, Sheng Q W, Feng M, Huang L G, Wang P, Jiang W S, Xing F, Liu Y G, Tian J G. Flexible graphene saturable absorber on two-layer structure for tunable mode-locked soliton fiber laser. Optics Express, 2014, 22(9): 10239–10247
17. Li D D, Zhu J W, Jiang M, Li D, Wu H, Han J, Sun Z P, Ren Z Y. Active-passive Q-switched fiber laser based on graphene microfiber. Applied Physics. B, Lasers and Optics, 2019, 125(11): 203
18. Wang Y R, Zhang B T, Yang H, Hou J, Su X C, Sun Z P, He J L. Passively mode-locked solid-state laser with absorption tunable graphene saturable absorber mirror. Journal of Lightwave Technology, 2019, 37(13): 2927–2931
19. Chai T, Li X, Feng T, Guo P, Song Y, Chen Y, Zhang H. Few-layer bismuthene for ultrashort pulse generation in a dissipative system based on an evanescent field. Nanoscale, 2018, 10(37): 17617–17622
20. Yan P, Lin R, Ruan S, Liu A, Chen H, Zheng Y, Chen S, Guo C, Hu J. A practical topological insulator saturable absorber for mode-locked fiber laser. Scientific Reports, 2015, 5(1): 8690
21. Mao D, Jiang B, Gan X, Ma C, Chen Y, Zhao C, Zhang H, Zheng J, Zhao J. Soliton fiber laser mode locked with two types of film-based Bi_2Te_3 saturable absorbers. Photonics Research, 2015, 3(2): A43
22. 22.Zhang Y, Li X, Qyyum A, Feng T, Guo P, Jiang J, Zheng H. PbS nanoparticles for ultrashort pulse generation in optical communication region. Particle & Particle Systems Characterization, 2018, 35 (11): 1800341
23. Hui Z, Xu W, Li X, Guo P, Zhang Y, Liu J. Cu_2S nanosheets for ultrashort pulse generation in the near-infrared region. Nanoscale, 2019, 11(13): 6045–6051
24. Wu M, Li X, Wu K, Wu D, Dai S, Xu T, Nie Q. All-fiber 2 μm thulium-doped mode-locked fiber laser based on MoS_2-saturable absorber. Optical Fiber Technology, 2019, 47: 152–157
25. Liu W, Pang L, Han H, Bi K, Lei M, Wei Z. Tungsten disulphide for ultrashort pulse generation in all-fiber lasers. Nanoscale, 2017, 9 (18): 5806–5811
26. Woodward R I, Howe R C T, Hu G, Torrisi F, Zhang M, Hasan T, Kelleher E J R. Few-layer MoS_2-saturable absorbers for short-pulse laser technology: current status and future perspectives. Photonics Research, 2015, 3(2): A30
27. Feng J, Li X, Shi Z, Zheng C, Li X, Leng D, Wang Y, Liu J, Zhu L. 2D ductile transition metal chalcogenides (TMCs): novel high-performance Ag_2S nanosheets for ultrafast photonics. Advanced Optical Materials, 2019: 1901762
28. Kong L, Qin Z, Xie G, Guo Z, Zhang H, Yuan P, Qian L. Black phosphorus as broadband saturable absorber for pulsed lasers from 1 μm to 2.7 μm wavelength. Laser Physics Letters, 2016, 13(4): 045801
29. Wei R, Wang M, Zhu Z, Lai W, Yan P, Ruan S, Wang J, Sun Z, Hasan T. High-power femtosecond pulse generation from an all-fiber Er-doped chirped pulse amplification system. IEEE Photonics Journal, 2020, 12(2): 3200208
30. Zhao C, Zhang H, Qi X, Chen Y, Wang Z, Wen S C, Tang D Y. Ultra-short pulse generation by a topological insulator based saturable absorber. Applied Physics Letters, 2012, 101(21): 211106
31. Fang J, Yang Z, long S, Wu Z, Zhao X, Liang F, Jiang Z, Chen Z. High-speed indoor navigation system based on visible light and mobile phone. IEEE Photonics Journal, 2017, 9(2): 8200711
32. Mao D, Cui X, Zhang W, Li M, Feng T, Du B, Lu H, Zhao J. Q-switched fiber laser based on saturable absorption of ferroferric-oxide nanoparticles. Photonics Research, 2017, 5(1): 52
33. Bai X, Mou C, Xu L, Wang S, Pu S, Zeng X. Passively Q-switched erbium-doped fiber laser using Fe_3O_4-nanoparticle saturable absorber. Applied Physics Express, 2016, 9(4): 042701
34. Chan C T. Photonic crystals and topological photonics. Frontiers of Optoelectronics, 2020, 13(1): 2–3
35. Li H, Ma B. Research development on fabrication and optical properties of nonlinear photonic crystals. Frontiers of Optoelectronics, 2020, 13(1): 35–49
36. Xing G, Jiang J, Ying J Y, Ji W. Fe_3O_4-Ag nanocomposites for optical limiting: broad temporal response and low threshold. Optics Express, 2010, 18(6): 6183–6190
37. Li N, Jia H, Liu J X, Cui L H, Jia Z X, Kang Z, Qin G S, Qin W P. Fe_3O_4 nanoparticles as the saturable absorber for a mode-locked fiber laser at 1558 nm. Laser Physics Letters, 2019, 16(6): 065102
38. Yang J, Hu J, Luo H, Li J, Liu J, Li X, Liu Y. Fe_3O_4 nanoparticles as a saturable absorber for a tunable Q-switched dysprosium laser around 3 μm. Photonics Research, 2020, 8(1): 70–77
39. Liu J S, Li X H, Qyyum A, Guo Y X, Chai T, Xu H, Jiang J. Fe_3O_4 nanoparticles as a saturable absorber for giant chirped pulse generation. Beilstein Journal of Nanotechnology, 2019, 10: 1065–1072
40. El-Diasty F, El-Sayed H M, El-Hosiny F I, Ismail M I M. Complex susceptibility analysis of magneto-fluids: optical band gap and surface studies on the nanomagnetite-based particles. Current Opinion in Solid State and Materials Science, 2009, 13(1–2): 28–34
41. Tang D Y, Zhao L M, Zhao B, Liu A Q. Mechanism of multisoliton formation and soliton energy quantization in passively mode-locked fiber lasers. Physical Review A, 2005, 72(4): 043816
42. Guo B, Yao Y, Tian J J, Zhao Y F, Liu S, Li M, Quan M R. Observation of bright-dark soliton pair in a fiber laser with topological insulator. IEEE Photonics Technology Letters, 2015, 27(7): 701–704
43. Zhang H, Tang D, Zhao L, Wu X. Dual-wavelength domain wall solitons in a fiber ring laser. Optics Express, 2011, 19(4): 3525–3530
44. Li X, Liu X, Hu X, Wang L, Lu H, Wang Y, Zhao W. Long-cavity passively mode-locked fiber ring laser with high-energy rectangular-shape pulses in anomalous dispersion regime. Optics Letters, 2010, 35(19): 3249–3251
45. Chang W, Ankiewicz A, Soto-Crespo J M, Akhmediev N. Dissipative soliton resonances in laser models with parameter management. Journal of Applied Physics, 2008, 25(12): 1972
46. Wang X, Xia Q, Gu B A. A 1.9 μm noise-like mode-locked fiber laser based on compact figure-9 resonator. Optics Communications, 2019, 434: 180–183
47. Bravo-Huerta E, Durán-Sánchez M, Álvarez-Tamayo R I, Santiago-Hernández H, Bello-Jiménez M, Posada-Ramírez B, Ibarra-Escamilla B, Pottiez O, Kuzin E A. Single and dual-wavelength noise-like pulses with different shapes in a double-clad Er/Yb fiber

laser. Optics Express, 2019, 27(9): 12349–12359
48. Wang S K, Ning Q Y, Luo A P, Lin Z B, Luo Z C, Xu W C. Dissipative soliton resonance in a passively mode-locked figure-eight fiber laser. Optics Express, 2013, 21(2): 2402–2407
49. Luo Z C, Cao W J, Lin Z B, Cai Z R, Luo A P, Xu W C. Pulse dynamics of dissipative soliton resonance with large duration-tuning range in a fiber ring laser. Optics letters, 2012, 37(22): 4777–4779
50. Liu L, Liao J H, Ning Q Y, Yu W, Luo A P, Xu S H, Luo Z C, Yang Z M, Xu W C. Wave-breaking-free pulse in an all-fiber normal-dispersion Yb-doped fiber laser under dissipative soliton resonance condition. Optics Express, 2013, 21(22): 27087–27092
51. Li X, Wang Y, Zhao W, Liu X, Wang Y, Tsang Y H, Zhang W, Hu X, Yang Z, Gao C, Li C, Shen D. All-fiber dissipative solitons evolution in a compact passively Yb-doped mode-locked fiber laser. Journal of Lightwave Technology, 2012, 30(15): 2502–2507
52. Jeong Y, Vazquez-Zuniga L A, Lee S, Kwon Y. On the formation of noise-like pulses in fiber ring cavity configurations. Optical Fiber Technology, 2014, 20(6): 575–592
53. Li X, Wang Y, Zhang W, Zhao W. Experimental observation of soliton molecules evolution in Yb-doped passively mode locked fiber lasers. Laser Physics Letters, 2014, 11(7): 075103

Xiaohui Li received a B.S. degree in Science from North-West University, Xi'an, China in 2006 and a Ph.D. degree from State Key Laboratory of Transient Optics and Photonics, Xi'an Institute of Optics and Precision Mechanics, Chinese Academy of Sciences, Xi'an, China in 2012. He is with School of Physics and Information Technology, Shaanxi Normal University, where he is currently a researcher. His current research interests include passively mode-locked fiber laser, high-power fiber laser, and solitons in fiber.

Jiajun Peng received a B.S. degree in Computer Science from Zhengzhou University, Zhengzhou, China in 2019. He is currently working toward an M.S. degree in Physics at School of Optical Engineering, Shaanxi Normal University, Xi'an, China. His current research interests include passively mode-locked fiber laser, high-power fiber laser, and solitons in fiber.

Jishu Liu received a Master's degree in Engineering from Shaanxi Normal University, Xi'an, China in 2020. His current research interests include passively mode-locked fiber laser and solitons in fiber.

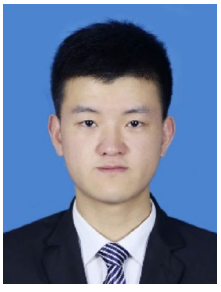

Tianci Feng received a B.S. degree in Science from Xianyang Normal University, China in 2017 and a Master's degree from Shaanxi Normal University, China in 2020. He majored in optics, and his current research interests include passively mode-locked fiber laser and 2D materials.

Cunxiao Gao received an M.S. degree in Optoelectronic Technology from North-West University, Xi'an, China in 2002 and a Ph.D. degree in Optics from Graduate University of Chinese Academy of Sciences, Beijing, China. His research interests include fiber laser, fiber amplifier, and fiber nonlinear optics.